

Article

The Effects of *P5CR* Gene Function of Endophytic Fungus *Alternaria oxytropis* OW7.8 on Swainsonine Biosynthesis

Fan Yang^{1,2,†} , Yinzhe Li^{1,2,†}, Ping Lu^{1,2,*}, Yu Wang^{1,2}, Feng Gao^{1,2}, Bo Yuan^{1,2}, Ling Du^{1,2}, Yuling Li^{1,2} and Kai Jiang^{1,2} 

¹ College of Life Science and Technology, Inner Mongolia Normal University, Hohhot 010022, China; atlas_yf@163.com (F.Y.); liyinzhe1@outlook.com (Y.L.); wangyu051606@163.com (Y.W.); imgaofeng@163.com (F.G.); yuanbo934@126.com (B.Y.); nmduling@163.com (L.D.); liyuling@163.com (Y.L.); jiangkai@imnu.edu.cn (K.J.)

² Key Laboratory of Biodiversity Conservation and Sustainable Utilization in Mongolian Plateau for College and University of Inner Mongolia Autonomous Region, Hohhot 010022, China

* Correspondence: luping@imnu.edu.cn

† These authors contributed equally to this work.

Abstract: Locoweeds, including *Oxytropis* and *Astragalus* species, are globally recognized as plants containing swainsonine (SW), a neurotoxic alkaloid that induces neurological dysfunction and growth inhibition in livestock. SW is produced by endophytic fungi in plants; the pyrroline-5-carboxylate reductase (*P5CR*) gene is critical in the fungal SW biosynthetic pathway. In this study, a *P5CR* gene knockout mutant ($\Delta P5CR$) was constructed from the endophytic fungus *Alternaria oxytropis* OW7.8 isolated from *Oxytropis glabra*. Compared to the wild-type strain (*A. oxytropis* OW7.8), the SW content in the $\Delta P5CR$ mycelia was significantly reduced, indicating that the *P5CR* gene plays a crucial role in promoting SW biosynthesis. Compared to the wild-type strain *A. oxytropis* OW7.8, the $\Delta P5CR$ mutant exhibited distinct morphological alterations in both colony and mycelial structures. The transcriptomic analysis of *A. oxytropis* OW7.8 and $\Delta P5CR$ revealed the downregulation of six genes associated with SW biosynthesis. Metabolomic profiling further demonstrated altered levels of six metabolites linked to SW synthesis. These findings provide foundational insights into the molecular mechanisms and metabolic pathways underlying SW biosynthesis in fungi. They hold significant value for future strategies to control SW in *Oxytropis glabra* and contribute positively to the protection and sustainable development of grassland ecosystems.

Keywords: *Alternaria oxytropis* OW 7.8; swainsonine; *P5CR* gene



Academic Editor: Kyoungwhan Back

Received: 1 March 2025

Revised: 20 March 2025

Accepted: 20 March 2025

Published: 21 March 2025

Citation: Yang, F.; Li, Y.; Lu, P.; Wang, Y.; Gao, F.; Yuan, B.; Du, L.; Li, Y.; Jiang, K. The Effects of *P5CR* Gene Function of Endophytic Fungus *Alternaria oxytropis* OW7.8 on Swainsonine Biosynthesis. *Biomolecules* **2025**, *15*, 460. <https://doi.org/10.3390/biom15040460>

Copyright: © 2025 by the authors. Licensee MDPI, Basel, Switzerland. This article is an open access article distributed under the terms and conditions of the Creative Commons Attribution (CC BY) license (<https://creativecommons.org/licenses/by/4.0/>).

1. Introduction

Locoweeds, globally referred to as *Oxytropis* and *Astragalus* species containing swainsonine (SW), are predominantly distributed in western China, North America, and Australia [1,2]. SW, an indolizidine alkaloid, inhibits intracellular mannosidase activity, leading to neurological dysfunction and growth inhibition in livestock upon ingestion [3–5]. Notably, SW also exhibits potential as an anticancer agent by activating mitochondrial-mediated apoptosis, suppressing tumor metastasis, and inducing cancer cell death [6–8]. To date, studies have confirmed that SW in locoweeds is biosynthesized by endophytic fungi of the genus *Alternaria* [9–13].

Endophytic fungi associated with locoweeds belong to *Alternaria* spp., including four species: *A. oxytropis*, *A. cinereum*, *A. fulva*, and *A. bornmuellerii* [14–16]. Early work by Braun

et al. isolated *Alternaria* endophytes from eight locoweed species, and Chinese researchers identified *A. oxytropis* in *Oxytropis kansuensis*, *O. glabra*, and *O. ochrocephala* [17–22]. Our research group first isolated *A. oxytropis* from *O. glabra* populations. This strain, designated *A. oxytropis* OW7.8, produces SW in vitro [23,24]. The saccharopine reductase (*sac*) catalyzes the following reaction in fungi: α -Amino adipic semialdehyde + glutamate + NADPH + H⁺ \leftrightarrow saccharopine + α -ketoglutarate + NADP⁺ + H₂O. Saccharopine is one of the intermediate compounds in SW biosynthesis. To investigate SW biosynthesis, we generated a *saccharopine reductase* gene (*sac*) knockout mutant M1 in *A. oxytropis* OW7.8 [23,24]. The M1 mutant exhibited a reduced SW level, while the complemented strain C1 had a higher SW level than both M1 and OW7.8, indicating that Sac enzyme activity promotes SW biosynthesis [23–25]. Furthermore, the supplementation of the culture medium with saccharopine, α -amino adipic acid, L-lysine, or L-pipecolic acid (L-PA) enhanced SW production in both wild-type OW7.8 and M1 strains. The transcriptomic analysis of *A. oxytropis* OW7.8 and the M1 mutant revealed key genes associated with SW biosynthesis [25]. Based on these findings, it is speculated that L-PA can originate from two branches: the delta-1-piperidine-2-carboxylate (P2C) branch and delta-1-piperidine-6-carboxylate (P6C) branch [23–25].

A comparative genomic analysis of 34 fungal species, including locoweed-associated *Alternaria* spp., human dermatophyte *Arthroderma* spp., and entomopathogenic *Metarhizium* spp., was conducted using Hidden Markov Models (HMMs) [12,26]. This analysis identified putative SW synthesis-related gene clusters (designated SWN gene clusters) and predicted the functional members involved in SW biosynthesis. The SWN cluster comprises seven genes (*swnA*, *swnH1*, *swnH2*, *swnK*, *swnN*, *swnR*, and *swnT*; Table 1), whose encoded enzymes primarily catalyze the conversion of L-PA to SW [12,26]. Intriguingly, the composition of the SWN cluster varies across fungal species. In locoweed endophytes, the cluster contains five core genes (*swnH1*, *swnH2*, *swnK*, *swnN*, and *swnR*), whereas *swnA* and *swnT* are absent [12,26].

Table 1. Members of the SWN gene clusters and their predicted functions [12,26].

Gene	Encoding Product	Function Prediction
<i>swnA</i>	Aminotransferase	Catalyzing the synthesis of pyrroline-6-carboxylate (P6C) from L-lysine
<i>swnR</i>	Dehydrogenase or reductase	Catalyzing the synthesis of L-PA from P6C
<i>swnK</i>	Multifunctional protein	Catalyzing the synthesis of 1-oxoindolizidine (or 1-hydroxyindolizidine) from L-PA
<i>swnN</i>	Dehydrogenase or reductase	Catalyzing the synthesis of 1-hydroxyindolizidine from 1-oxoindolizidine
<i>swnH1</i>	Fe(II)/ α -Ketoglutarate-dependent dioxygenase	Catalyzing the synthesis of SW from 1,2-dihydroxyindolizidine
<i>swnH2</i>	Fe(II)/ α -Ketoglutarate-dependent dioxygenase	Catalyzing the synthesis of 1,2-dihydroxyindolizidine from 1-hydroxyindolizidine
<i>swnT</i>	Transmembrane transporter	Transport of SW

Our research team previously cloned the *swnN* gene (GenBank: OR596336) and the *swnH1* gene (GenBank: ON416998) from *A. oxytropis* OW7.8 [27,28]. The *swnN* and *swnH1* genes were individually knocked out in *A. oxytropis* OW7.8, and SW was undetectable in both $\Delta swnN$ and $\Delta swnH1$ mutants [27,28]. However, the complemented strain $\Delta swnN/swnN$ regained the ability to synthesize SW, indicating that *swnN* and *swnH1* genes promote SW biosynthesis [27,28]. Transcriptomic and metabolomic analyses of OW7.8 and $\Delta swnN$ predicted six genes (*sac*, *P5CR*, *swnH1*, *swnK*, *swnH2*, and *swnR*) and five metabolites (L-glutamate, α -ketoglutaric acid, L-proline, 2-amino adipic acid, and L-PA) associated with SW biosynthesis [27]. Similarly, transcriptomic and metabolomic analyses of OW7.8 and $\Delta swnH1$

predicted five genes (*sac*, *swnN*, *swnK*, *swnH2*, and *swnR*) and five metabolites (α -aminoadipic acid, L-stachydrine, L-proline, saccharopine, and L-PA) linked to SW biosynthesis [28].

Early investigations into fungal SW biosynthesis primarily focused on *Rhizoctonia leguminicola* [13]. In this species, the SW biosynthetic pathway proceeds as follows: L-lysine is first reduced to saccharopine, which is subsequently converted to α -aminoadipic acid semialdehyde via the action of Sac. Following conformational rearrangement, α -aminoadipic acid semialdehyde generates P6C. P6C is then reduced to L-PA by 6-carboxyl-pipecolic acid reductase. L-PA undergoes reductive cyclization to form 1-oxoindolizidine, which is further reduced by 1-oxoindolizidine reductase to yield 1-hydroxyindolizidine. Subsequent reactions produce 1,2-dihydroxyindolizidine, which is ultimately hydroxylated to form SW (Figure 1) [13].

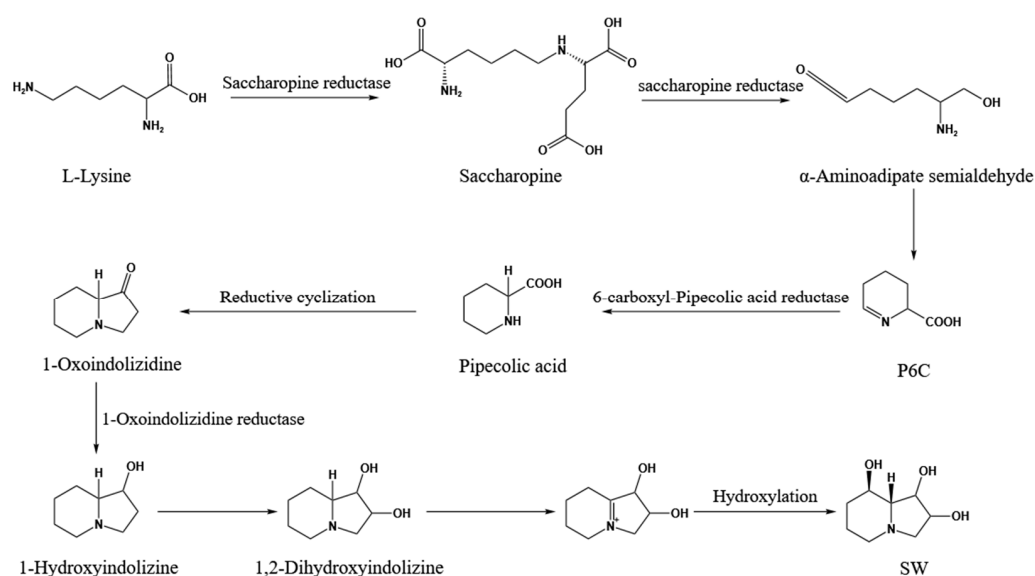


Figure 1. Partial biosynthesis pathways of SW from *R. leguminicola* [13].

In *Metarhizium robertsii*, the proposed biosynthetic pathway from L-PA to SW involves sequential enzymatic steps mediated by the *SWN* gene cluster [12]. L-PA and malonyl-CoA are initially condensed by the multifunctional protein SwnK, followed by reductive modifications catalyzed by SwnR or SwnN, yielding 1-hydroxyindolizidine intermediates. Subsequent hydroxylation by SwnH1 and SwnH2, coupled with further reduction by SwnR/SwnN, ultimately generates SW (Figure 2) [12].

To delineate the roles of *SWN* cluster members, knockout experiments were performed in *M. robertsii* [29]. These studies revealed two potential pathways for L-PA biosynthesis from L-lysine: L-Lysine is converted to P6C via the lysine aminotransferase (LAT/SwnA), which is subsequently reduced to L-PA by the reductase SwnR. L-Lysine undergoes direct cyclization to L-PA through lysine cyclodeaminase (LCD). The L-PA-derived intermediates then converge into a unified pathway: SwnK facilitates the condensation of L-PA with malonyl-CoA, generating (8aS)-1-oxoindolizidine. This intermediate is reduced by SwnN to form stereoisomers (1S,8aS)-1-hydroxyindolizidine and (1R,8aS)-1-hydroxyindolizidine. SwnH2 catalyzes the hydroxylation of these isomers, producing (1R,2S,8aS)-1,2-dihydroxyindolizidine, (1S,2S,8aS)-1,2-dihydroxyindolizidine, or (1S,2R,8aS)-1,2-dihydroxyindolizidine. Finally, 1,2-dihydroxyindolizidine undergoes hydroxylation to form SW (Figure 3) [29].

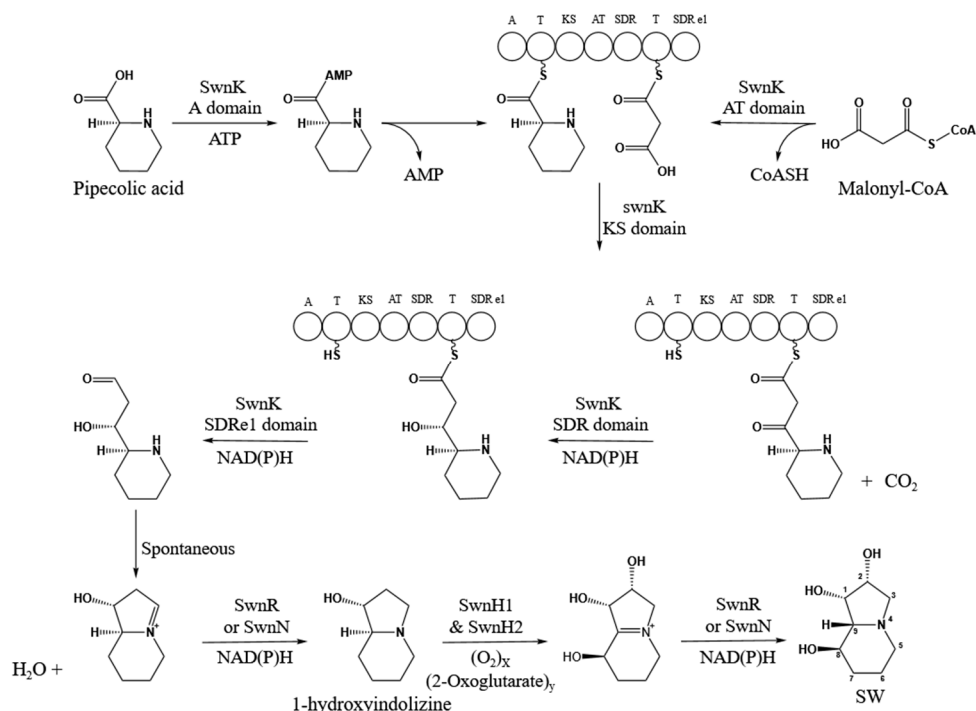


Figure 2. Partial biosynthesis pathways of SW in *M. robertsii* [12].

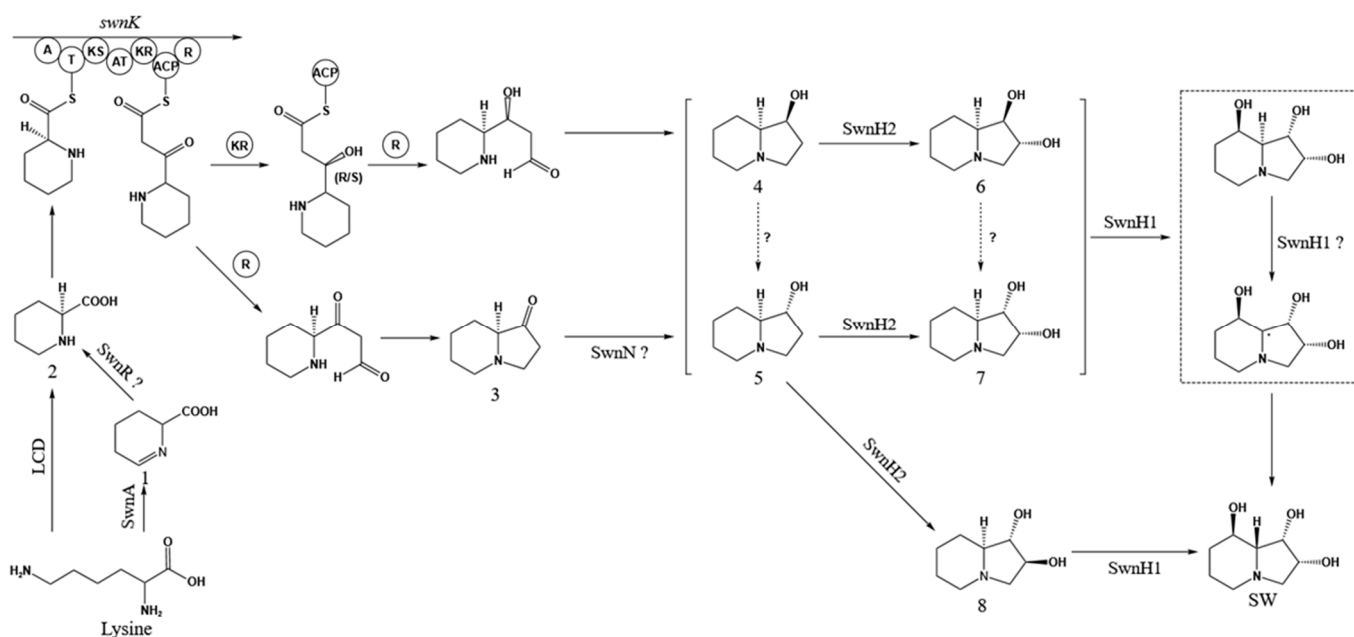


Figure 3. Biosynthesis pathways of SW in *M. robertsii* [29].

The *P5CR* gene (pyrroline-5-carboxylate reductase gene, *P5CR*) encodes pyrroline-5-carboxylate reductase (P5CR), which catalyzes the conversion of P6C to L-PA in fungi [30,31]. L-PA is recognized as a critical precursor for SW biosynthesis and serves as a key intermediate in the secondary metabolism of plants and microorganisms [32,33]. Notably, a limited number of studies have proposed that the *P5CR* gene in *A. oxytropis* from *O. ochrocephala* may also belong to the SWN cluster [21]. The transcriptomic analysis of OW7.8 and the M1 mutant revealed the downregulation of the *P5CR* gene in M1 compared to the wild-type strain, suggesting a potential regulatory role of *P5CR* in SW biosynthesis [23]. Our team previously

cloned the *P5CR* gene from the endophytic fungus *Alternaria oxytropis* OW7.8 (GenBank accession number: ON004912).

This study aims to investigate the role of the *P5CR* gene in SW biosynthesis in *Alternaria oxytropis* OW7.8 by constructing a *P5CR* knockout mutant ($\Delta P5CR$). The SW levels in both wild-type *A. oxytropis* OW7.8 and the $\Delta P5CR$ mutant will be quantified, followed by comprehensive transcriptomic and metabolomic analyses. These experiments are designed to elucidate the functional contribution of *P5CR* to the SW biosynthetic pathway in *A. oxytropis* OW7.8 and to refine the overall understanding of SW biosynthesis in this endophytic fungus. The findings of this research will provide critical insights into the molecular mechanisms and metabolic pathways underlying the fungal SW synthesis. Furthermore, this study holds significant practical value for guiding SW control strategies in locoweeds and contributes positively to the conservation and sustainable management of grassland ecosystems.

2. Materials and Methods

2.1. Fungal Strain

The *A. oxytropis* OW7.8 strain was isolated from *O. glabra* by our research group [34]. The mycelia were cultured on potato dextrose agar (PDA) medium at 25 °C for subsequent experiments.

2.2. Genomic DNA Extraction from *A. oxytropis* OW7.8

Genomic DNA was extracted from *A. oxytropis* OW7.8 using a plant genomic DNA extraction kit (TIANGEN). The quality of the extracted DNA was assessed by 1% agarose gel electrophoresis and quantified using a Q5000 spectrophotometer (Quawell).

2.3. Construction of the *P5CR* Gene Knockout Vector

The upstream and downstream homologous sequences of the *P5CR* gene were amplified using *A. oxytropis* OW7.8 genomic DNA as the template and P5CR-UF/P5CR-UR (5'-CGCGGATCCATGGCAAACACGCAGGAATCTAAGC-3'; 5'-GCACCGGTGTCACAGGCGATGAAGTTGGAGAG-3') and P5CR-DF/P5CR-DR (5'-TATCCTGCAGGCTCAGCGAGGCGCAGTACAAGCTT-3'; 5'-CGGAATTCCTACCGCCTGTGGTTCACGA-3') as primers. The hygromycin phosphotransferase gene (*hpt*) was amplified using the pCT74 plasmid (MiaoLingBio) as the template and H-F/H-R (5'-GCACCGGTGGCTTGGCTGGAGCTAGTGGAGGTC-3'; 5'-CGGCCTGCAGGGAACCCGCGGTCCGGCATCTACTCTAT-3') as primers. Using restriction enzyme digestion and ligation, the upstream and downstream homologous sequences of *P5CR* were flanked to the *hpt* gene, constructing the *P5CR* knockout cassette. This cassette was then ligated into the pUC19 vector (Takara) to generate the *P5CR* gene knockout vector.

2.4. Protoplast Preparation and Transformation of *A. oxytropis* OW7.8

Young mycelia of *A. oxytropis* OW7.8 were inoculated into 150 mL of potato dextrose broth (PDB) medium and cultured at 180 rpm and 25 °C for approximately 5 days. The protoplast lysis solution was prepared by dissolving 0.3 g Driselase, 0.1 g Lysing Enzyme, and 0.004 g Chitinase in a 15 mL centrifuge tube containing a small volume of 1.2 mol/L MgSO₄ solution, which was then adjusted to a final volume of 10 mL. The mixture was shaken at 80 rpm and 30 °C for 30 min and filtered through a 0.22 µm organic filter into a 50 mL centrifuge tube. Mycelial balls were filtered through a Miracloth (22–25 µm pore size) funnel, rinsed twice with ddH₂O and once with 1.2 mol/L MgSO₄, and gently squeezed before being added to the lysis solution. The mixture was incubated at 80 rpm and 30 °C for 4 h. After incubation, the solution was filtered through Miracloth into a new 50 mL centrifuge tube, rinsed twice with 1.2 mol/L MgSO₄, and centrifuged at

4000 rpm for 5 min. The supernatant was discarded, and the pellet was resuspended in 5 mL of STC buffer (1 mol/L Sorbitol, 100 mmol/L CaCl₂, 100 mmol/L Tris-HCl), followed by centrifugation at 4000 rpm for 5 min. The pellet was resuspended in an appropriate volume of STC buffer, and the protoplasts were aliquoted into 100 µL portions. Approximately 2 µg of the *P5CR* knockout vector was added to each tube, mixed gently, and incubated on ice for 25 min. SPTC buffer (prepared fresh by adding 0.4 g PEG8000 to 1 mL STC) was filter-sterilized using a 0.22 µm organic filter. One milliliter of SPTC buffer was added to each tube, mixed gently, and incubated at room temperature for 30 min. After centrifugation at 4000 rpm for 5 min, the supernatant was discarded. Each tube was mixed with 12.5 mL of molten 1.5% TB3 regeneration medium (1 mol/L Sucrose, 0.3% Yeast Extract, 0.3% Casein, 1.5% Agarose L.M.P) containing 50 µg/mL ampicillin (Amp) and 1 µg/mL hygromycin B (Hyg B), poured into plates, and incubated overnight at 25°C. Molten 0.7% TB3 regeneration medium (1 mol/L Sucrose, 0.3% Yeast Extract, 0.3% Casein, 0.7% Agarose L.M.P) supplemented with 50 µg/mL Amp and 2 µg/mL Hyg B was added to the plates and incubated at 25 °C for approximately 14 days.

2.5. Screening and Identification of Transformants

Transformants resistant to Hyg B were screened and verified by PCR. Genomic DNA from transformants was used as the template for amplification with the following primer pairs: hptF/hptR (5'-GGCTTGCTGGAGCTAGTGGAGGTC-3'; 5'-GAACCCGCGGTCGG CATCTACTCTAT-3') for the *hpt* sequence, P5CR-TF/hptR (5'-ATCCGAACCGTCCAAG-3'; 5'-GAACCCGCGGTCGGCATCTACTCTAT-3') for the upstream homologous sequence plus *hpt*, P5CR-TF/P5CR-TR (5'-ATCCGAACCGTCCAAG-3'; 5'-AAGTCCAGTGGTTCCT CTCAT-3') for the *P5CR* knockout cassette, and HYP-F/HYP-R (5'-GACATCGTGCTGCTGA GTT-3'; 5'-GGTCCATCGGGATACAAG-3') for the internal *P5CR* sequence. PCR products were analyzed by gel electrophoresis and sequenced for validation (Sangon Biotech, Shanghai, China).

2.6. Scanning Electron Microscopy of Mycelia

The colony morphology of OW7.8 and $\Delta P5CR$ after 20 days of culture was observed. Mycelial morphology was examined using a scanning electron microscope (SU8100, 3.0 kV, $\times 30$, Hitachi, Tokyo, Japan).

2.7. Extraction and Detection of SW in *A. oxytropis* OW7.8 and $\Delta P5CR$ Mycelia

Mycelia from 20-day cultures of *A. oxytropis* OW7.8 and $\Delta P5CR$ were extracted using an acetic acid–chloroform solution. SW was purified using cation exchange resin and eluted with 1 mol/L ammonia. SW levels were quantified by HPLC-MS, with three replicates per sample. Data were analyzed using one-way ANOVA in GraphPad Prism 9.5.

2.8. Transcriptome Sequencing and Analysis of *A. oxytropis* OW7.8 and $\Delta P5CR$

Mycelia from 20-day cultures of *A. oxytropis* OW7.8 and $\Delta P5CR$ were flash-frozen in liquid nitrogen and stored on dry ice for sequencing. Three biological replicates were prepared for each strain. Transcriptome sequencing was performed on the Illumina NovaSeq 6000 platform (Novogene, Beijing, China). Data analysis was conducted using the R packages DESeq2 and clusterProfiler, with differentially expressed genes (DEGs, $|\log_2(\text{Fold Change})| \geq 1$ and $\text{padj} \leq 0.05$) subjected to KEGG and GO functional enrichment analysis [35–37].

2.9. Metabolomic Profiling and Analysis of *A. oxytropis* OW7.8 and $\Delta P5CR$

Mycelia from 20-day cultures of *A. oxytropis* OW7.8 and $\Delta P5CR$ were flash-frozen in liquid nitrogen and stored on dry ice for metabolomic analysis. Five biological replicates were prepared for each strain. Metabolites were detected using HPLC-MS² technology

(Novogene, Beijing, China). Data analysis was performed using the R package Compound Discoverer, and differentially metabolites ($VIP > 1$, $|\log_2(\text{Fold Change})| \geq 0.59$ and $p\text{-value} < 0.05$) were subjected to KEGG functional enrichment analysis [38–40].

2.10. Extraction of SW Biosynthesis-Related Gene Expression Levels in *A. oxytropis* OW7.8 and $\Delta P5CR$

Total RNA was extracted from *A. oxytropis* OW7.8 and $\Delta P5CR$ using the OminiPlant RNA Kit (CW BIO) and reverse-transcribed into cDNA. RT-qPCR was performed using cDNA templates from both strains, with the actin gene as the internal reference. The following primer pairs were used to amplify six SW biosynthesis-related genes: sac-F/sac-R (5'-CTGCTGCTCGGTGCTGGATTC-3'; 5'-CTAGACTGATGGCGTTGGTGTGG-3'); R-F/R-R (5'-TTCTACTTTGCCACACACGAACCC-3'; 5'-ATAGTCAGCCAACCAGCCAATGC-3'); K-F/K-R (5'-GACCGCTTGCTCGCCTGTG-3'; 5'-CTCGTCAACTCGTCCAACACTTCC-3'); N-F/N-R (5'-TGACTAAGTTCATTCCCAGCG-3'; 5'-AAGAGTTCGGTTTCTGCCTC-3'); H2-F/H2-R (5'-CATCTGCTCCTCGCTTGCTACC-3'; 5'-CAGGACAACGCCTCCATCTCTTTC-3'); H1-F/H1-R (5'-TTGCTTTGCGGAGATGGAACCAG-3'; 5'-CGGAGTGTGCCTGAGATGAAGAAG-3'). Gene expression levels were statistically analyzed using GraphPad Prism 9.5.0, with one-way ANOVA applied to compare data across sample groups.

3. Results

3.1. Construction of the *P5CR* Gene Knockout Vector in *A. oxytropis*

The upstream and downstream homologous sequences of the *P5CR* gene and the *hpt* gene were successfully amplified (Figure 4A). These three fragments were ligated to construct the *P5CR* knockout cassette, which was then inserted into the pUC19 vector to generate the *P5CR* knockout vector (Figure 4B). The final vector contained the ampicillin resistance gene (*Amp^R*) and the *P5CR* knockout cassette, which included the *hpt* gene.

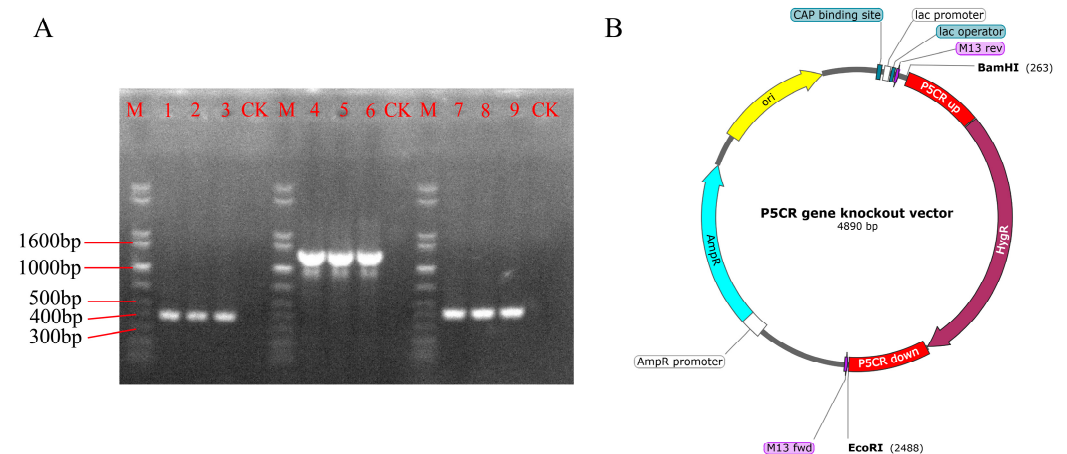


Figure 4. Construction of the *P5CR* gene knockout vector. Note: M: 1 kb plus DNA ladder. (A) PCR electrophoresis image of the upstream and downstream homologous sequences of the *P5CR* gene and the *hpt* gene. Lane 1, 2, 3: Upstream homologous sequence of the *P5CR* gene, expected product: 422 bp. Lane 4, 5, 6: *hpt* gene sequence, expected product: 1398 bp. Lane 7, 8, 9: Downstream homologous sequence of the *P5CR* gene, expected product: 439 bp. CK: Negative control. (B) Schematic diagram of the *P5CR* gene knockout vector. Original Images for Gels see Supplementary Materials.

3.2. Screening and Identification of Knockout Transformants

One week after transforming the *A. oxytropis* OW7.8 protoplasts with the knockout vector, a small number of transformants appeared on the TB3 medium. These transformants were transferred to a PDA medium supplemented with 2 $\mu\text{g}/\text{mL}$ of hygromycin B (Hyg

B) for resistance screening. The PCR analysis confirmed that the knockout strain $\Delta P5CR$ could amplify the *hpt* gene, the upstream homologous sequence of *P5CR* plus the *hpt* gene, and the *P5CR* knockout cassette, but not the internal sequence of *P5CR* (Figure 5). The sequencing of the PCR products further validated the correct integration of the knockout cassette, confirming the successful generation of the $\Delta P5CR$ mutant.

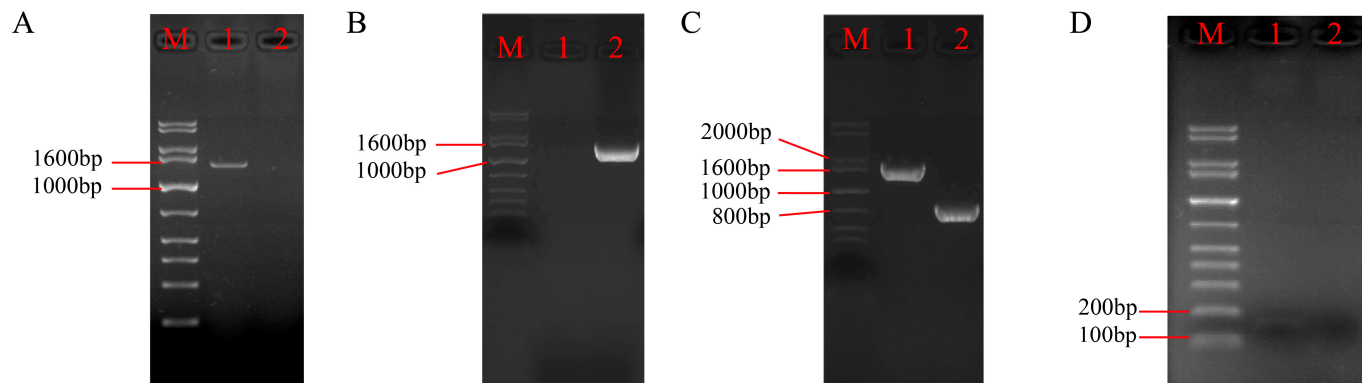


Figure 5. PCR electrophoresis images of transformants. Note: M: 1 kb plus DNA ladder (A) PCR amplification of the *hpt* gene sequence, expected product: 1380 bp. Lane 1: Transformant DNA; Lane 2: Wild-type strain DNA. (B) PCR amplification of the upstream homologous sequence of the *P5CR* gene + *hpt* gene sequence, expected product: 1563 bp. Lane 1: Wild-type strain DNA; Lane 2: Transformant DNA. (C) PCR amplification of the *P5CR* gene knockout cassette sequence, expected product: 759 bp for the wild-type strain and 1799 bp for the knockout strain. Lane 1: Transformant DNA; Lane 2: Wild-type strain DNA. (D) PCR amplification of the internal sequence of the *P5CR* gene, expected product: 152 bp. Lane 1: Wild-type strain DNA; Lane 2: Transformant DNA. Original Images for Gels see Supplementary Materials.

3.3. Comparison of Colony Morphology and Scanning Electron Microscopy (SEM) Structures Between *A. oxytropis* OW7.8 and $\Delta P5CR$

The wild-type *A. oxytropis* OW7.8 exhibited white, fluffy colonies with a raised center and radial mycelial growth, accompanied by melanin accumulation on the reverse side. In contrast, the $\Delta P5CR$ mutant formed raised, irregularly edged colonies with a creamy-white to pale-yellow appearance, lacking pigment accumulation. The mutant also displayed slower growth, irregular mycelial patterns, and densely packed, stacked hyphae (Figure 6).

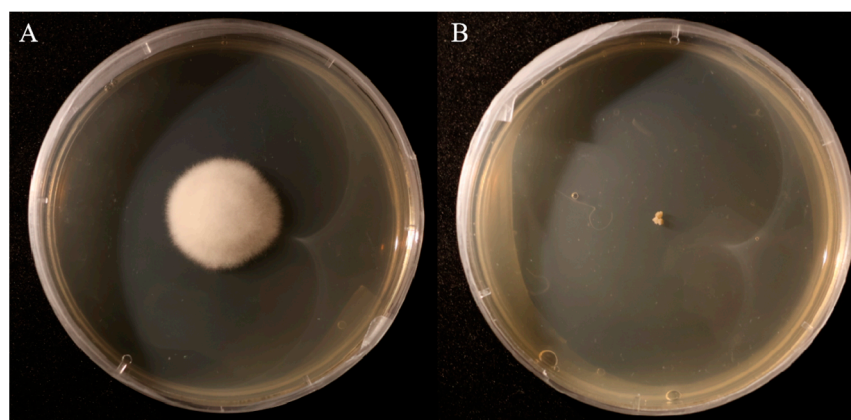


Figure 6. Colonies of *A. oxytropis* OW7.8 and $\Delta P5CR$. Note: (A) *A. oxytropis* OW7.8 (B) $\Delta P5CR$.

The SEM analysis revealed distinct morphological differences between the two strains. The wild-type *A. oxytropis* OW7.8 exhibited typical fungal mycelial structures, with loose, filamentous, and well-organized hyphae (Figure 7A,B). In contrast, the $\Delta P5CR$ mutant showed

an abnormal mycelial morphology, characterized by tightly packed, swollen, and irregularly shaped hyphae, with some structures appearing shrunken or collapsed (Figure 7C,D).

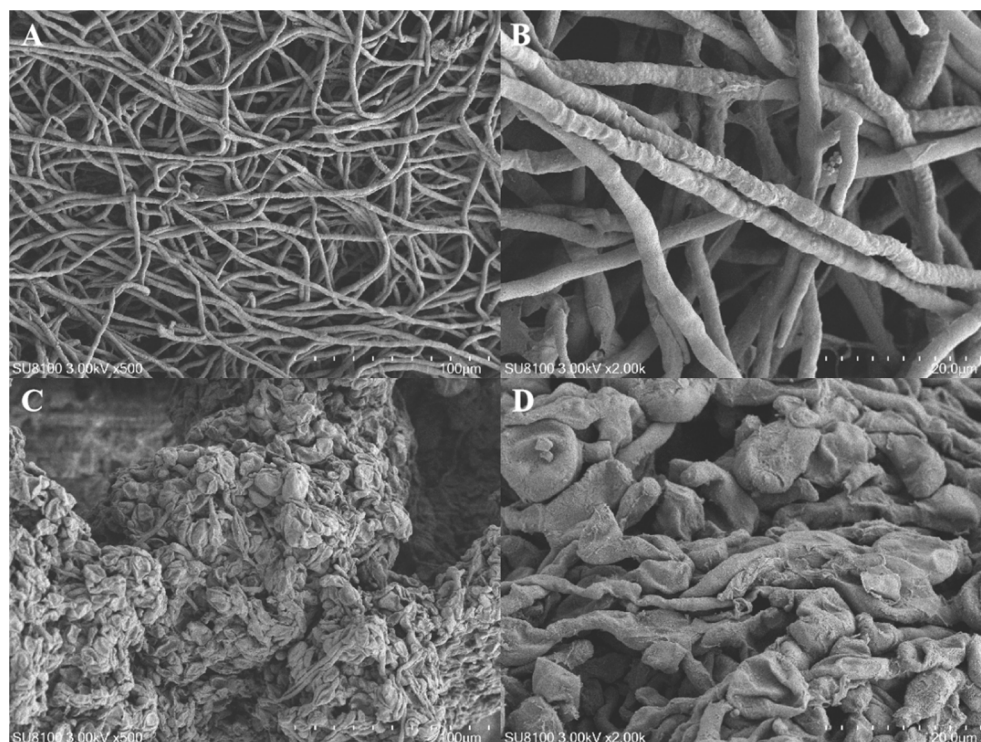


Figure 7. SEM Images of *A. oxytropis* OW7.8 and $\Delta P5CR$. Note: (A) SEM image of *A. oxytropis* OW7.8 (500 \times). (B) SEM image of *A. oxytropis* OW7.8 (2000 \times). (C) SEM image of $\Delta P5CR$ (500 \times). (D) SEM image of $\Delta P5CR$ (2000 \times).

3.4. SW Levels in *A. oxytropis* OW7.8 and $\Delta P5CR$ Mycelia

The SW content in 20-day-old mycelia of *A. oxytropis* OW7.8 was $102.69 \pm 3.38 \mu\text{g/g}\cdot\text{DW}$, while that in $\Delta P5CR$ was significantly lower at $46.82 \pm 7.41 \mu\text{g/g}\cdot\text{DW}$ ($p < 0.001$) (Figure 8).

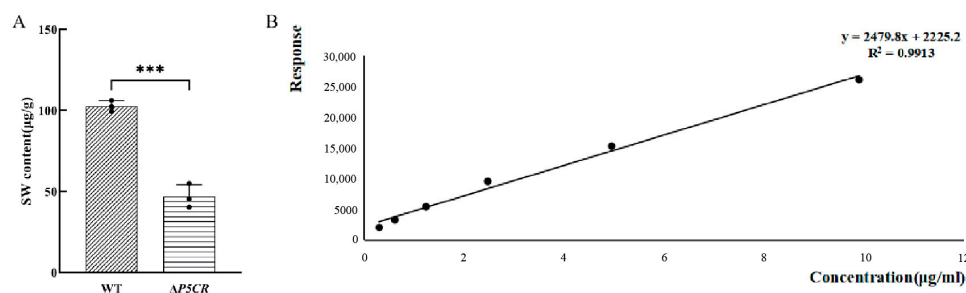


Figure 8. SW Levels in *A. oxytropis* OW7.8 and $\Delta P5CR$. Note: (A) SW levels in mycelia (***: $p < 0.001$). (B) Standard curve for SW level detection, with the standard equation: $y = 2479.8x + 2225.2$, $R^2 = 0.9913$.

3.5. Transcriptomic Analysis of *A. oxytropis* OW7.8 and $\Delta P5CR$

Transcriptome sequencing of *A. oxytropis* OW7.8 and $\Delta P5CR$ yielded 252,427,347 clean reads. Significant expression differences were observed between OW7.8 and $\Delta P5CR$ (Figure 9A), with 2791 differentially expressed genes (DEGs) identified, including 1273 upregulated and 1518 downregulated genes (Figure 9B).

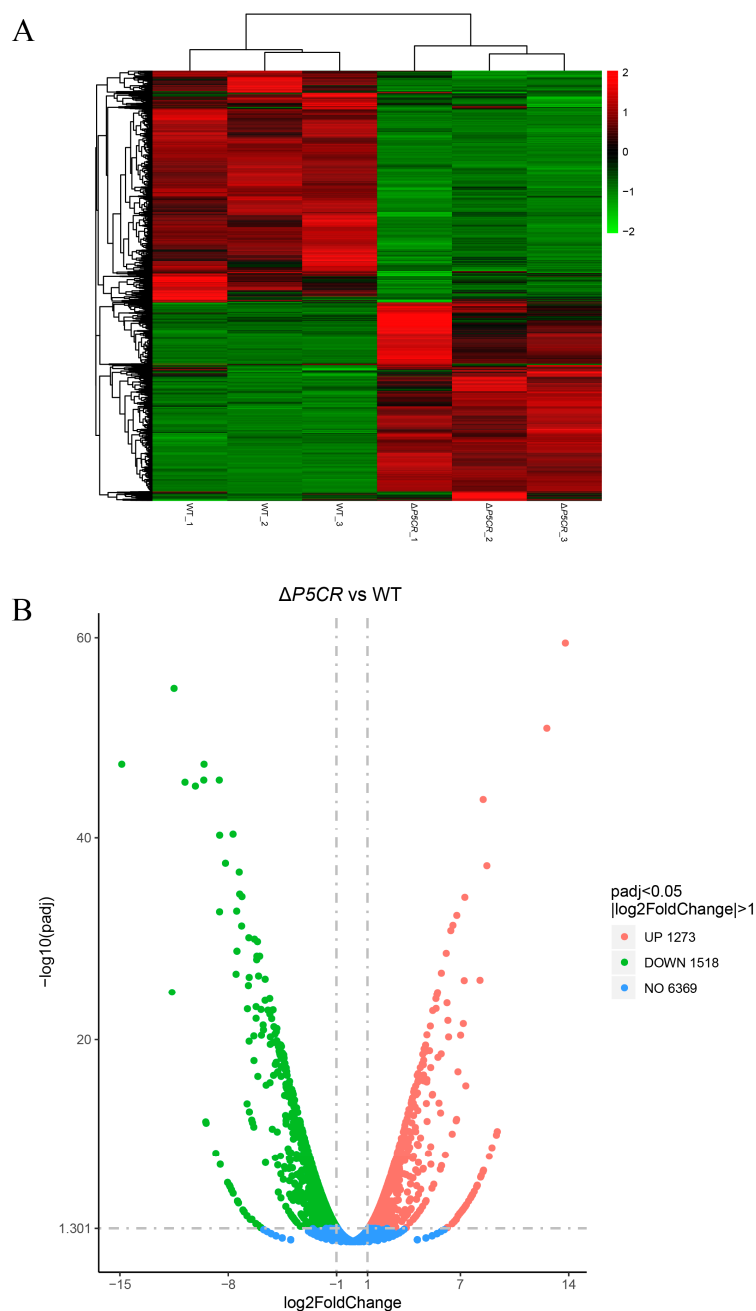


Figure 9. Transcriptome analysis of *A. oxytropis* OW7.8 and $\Delta P5CR$. Note: (A) Heatmap of clustered DEGs between the two groups. (B) Volcano plot of differential comparisons.

The GO enrichment analysis annotated 1535 DEGs to 582 biological processes (BPs), 183 cell components (CCs), and 770 molecular functions (MFs). Key enriched processes included an oxidation-reduction process, transmembrane transport, membrane part, intrinsic component of membrane, oxidoreductase activity, and cofactor binding (Figure 10A). Specifically, for the oxidation-reduction process, 55 genes were upregulated and 122 genes were downregulated; for oxidoreductase activity, 50 genes were upregulated and 117 genes were downregulated; for transmembrane transport, 41 genes were upregulated and 100 genes were downregulated; for cofactor binding, 47 genes were upregulated and 87 genes were downregulated; and for transmembrane transporter activity, 25 genes were upregulated and 69 genes were downregulated.

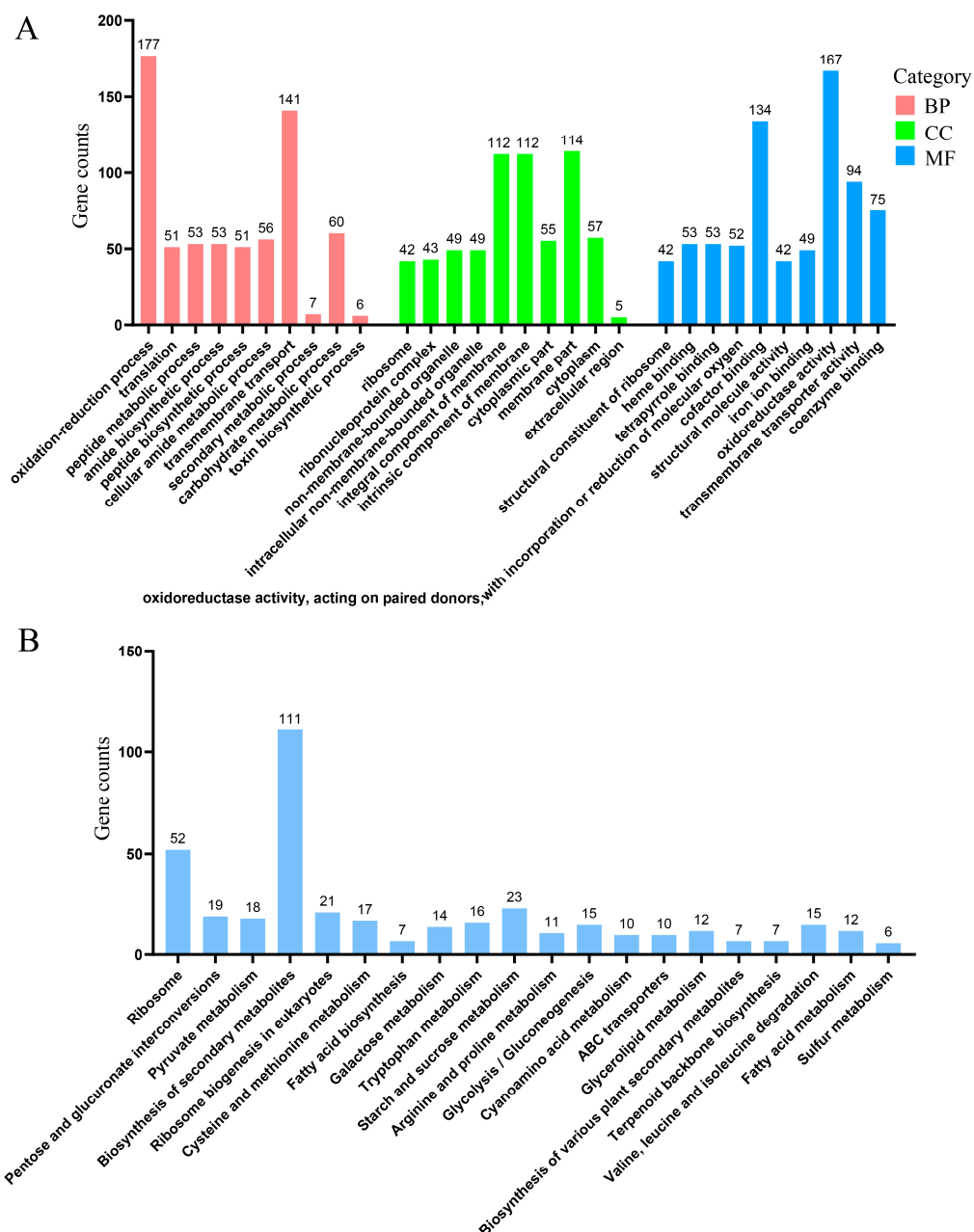


Figure 10. Transcriptome analysis of *A. oxytropis* OW7.8 and $\Delta P5CR$. Note: (A) GO functional classification annotation. (B) KEGG enrichment analysis.

The KEGG enrichment analysis annotated 893 DEGs, with the largest proportions associated with secondary metabolism and ribosome biosynthesis. Key pathways included ribosome, starch and sucrose metabolism, ribosome biogenesis in eukaryotes, and pentose and glucuronate interconversions (Figure 10B). Specifically, for the biosynthesis of secondary metabolites, 44 genes were upregulated and 67 genes were downregulated. For the ribosome, fifty-one genes were upregulated and one gene was downregulated. For starch and sucrose metabolism: five genes upregulated and eighteen genes were downregulated. For ribosome biogenesis in eukaryotes, twenty genes were upregulated and one gene was downregulated. For pentose and glucuronate interconversions, three genes were upregulated and sixteen genes were downregulated.

Notably, the expression levels of *swnN*, *swnR*, *swnK*, *swnH1*, *Amino adipate reductase*, and *sac* were downregulated in $\Delta P5CR$.

3.6. Metabolomic Profiling of *A. oxytropis* OW7.8 and $\Delta P5CR$

The principal component analysis (PCA) of metabolomic data revealed distinct metabolite profiles between $\Delta P5CR$ and OW7.8 (Figure 11A,B). In positive ion mode, the most abundant metabolites were lipids and lipid-like molecules (30.07%), followed by phenylpropanoids and polyketides (3.44%) and alkaloids and derivatives (2.17%). In negative ion mode, lipids and lipid-like molecules accounted for 39.14%, while phenylpropanoids and polyketides represented 2.53% (Figure 11C,D). A total of 498 differentially expressed metabolites (317 upregulated, 191 downregulated) were detected in positive ion mode, and 269 (159 upregulated, 110 downregulated) were detected in negative ion mode (Figure 12A,B).

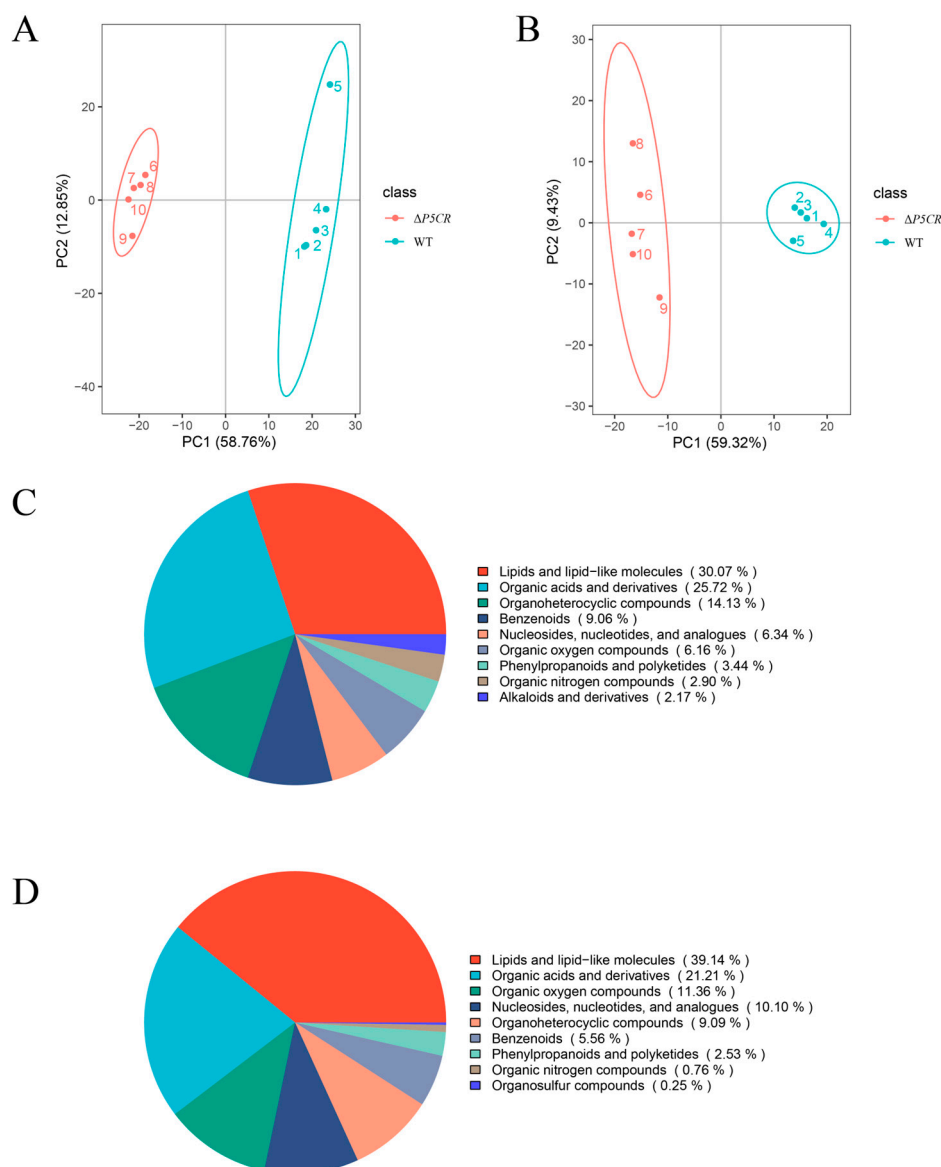


Figure 11. Metabolomic analysis of *A. oxytropis* OW7.8 and $\Delta P5CR$. Note: (A) Principal component analysis (PCA) in positive ion mode. (B) Principal component analysis (PCA) in negative ion mode. (C) Metabolite classification pie chart in positive ion mode. (D) Metabolite classification pie chart in negative ion mode.

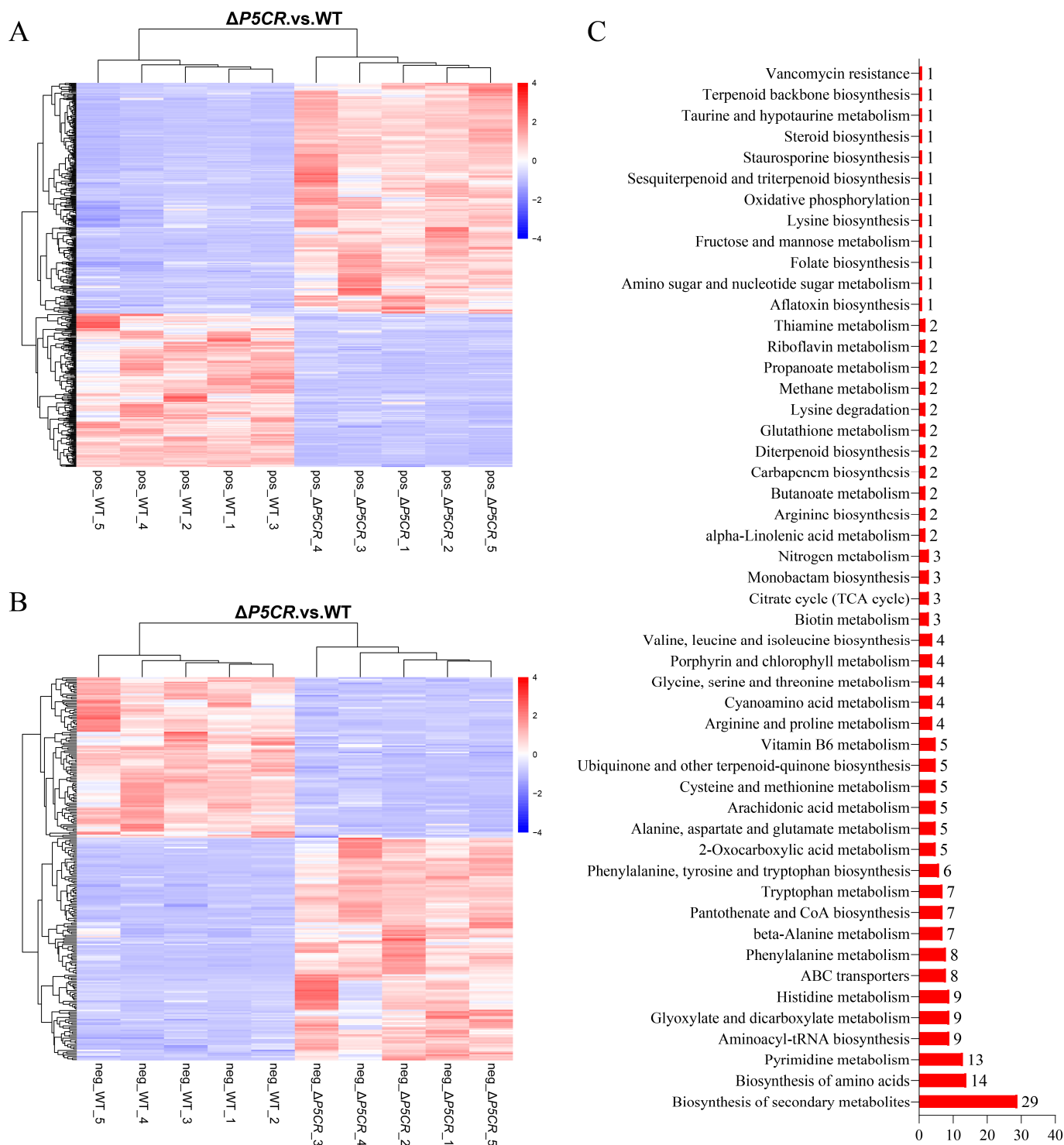


Figure 12. Metabolomic analysis of *A. oxytropis* OW7.8 and $\Delta P5CR$. Note: **(A)** Clustering heatmap analysis of differential metabolites in positive ion mode. **(B)** Clustering heatmap analysis of differential metabolites in negative ion mode. **(C)** KEGG enrichment analysis of differential metabolites.

The KEGG enrichment analysis of 777 differential metabolites annotated 222 metabolites to 50 metabolic pathways. These include the biosynthesis of secondary metabolites (twenty-nine), biosynthesis of amino acids (fourteen), Pyrimidine metabolism (thirteen), Aminoacyl-tRNA biosynthesis (nine), and Glyoxylate and dicarboxylate metabolism (nine) (Figure 12C). Six metabolites closely associated with SW biosynthesis were identified: saccharopine, L-PA, α -amino adipic acid, L-lysine, L-proline, and L-glutamate. Among these,

saccharopine, L-PA, α -aminoadipic acid, L-lysine, and L-proline were downregulated, while L-glutamate was upregulated.

3.7. Expression of SW Biosynthesis-Related Genes in *A. oxytropis* OW7.8 and $\Delta P5CR$

The RT-qPCR analysis of 20-day-old cultures revealed that the expression levels of *sac*, *swnR*, *swnK*, *swnN*, and *swnH1* were significantly lower in $\Delta P5CR$ compared to *A. oxytropis* OW7.8 ($p < 0.001$). No significant difference was observed in the expression of *swnH2* (Figure 13).

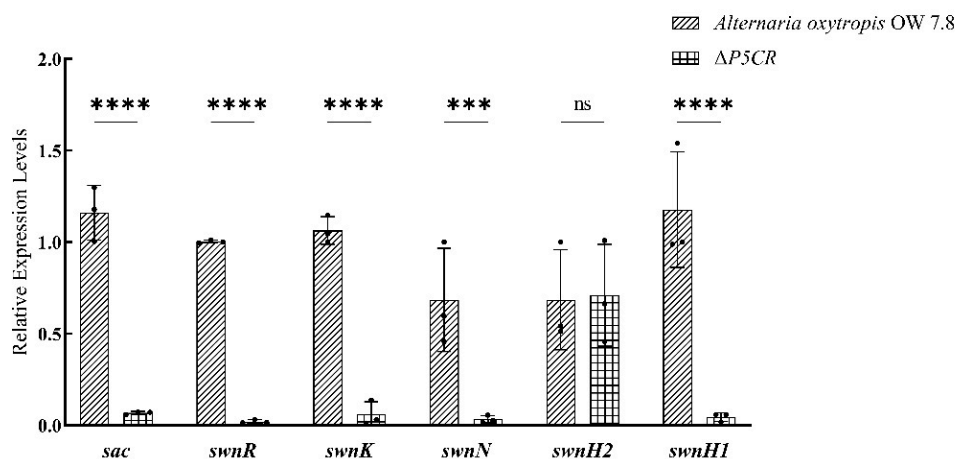


Figure 13. Expression of SWN gene cluster members and *sac* Gene in *A. oxytropis* OW7.8 and $\Delta P5CR$. Note: X-axis: gene names; Y-axis: relative gene expression levels; significance levels: *** $p < 0.0001$, **** $p < 0.00001$, ns $p > 0.05$.

4. Discussion

This study investigated the role of the *P5CR* gene in SW biosynthesis in the locoweed endophytic fungus *A. oxytropis* OW7.8. For the first time, we successfully knocked out the *P5CR* gene in *A. oxytropis* OW7.8, resulting in a significant reduction in SW levels in the $\Delta P5CR$ mutant compared to the wild-type strain. This finding indicates that *P5CR* enzyme activity promotes SW biosynthesis in fungi. Additionally, the $\Delta P5CR$ mutant exhibited slower growth, lack of pigment accumulation, irregular colony edges, and densely packed, swollen hyphae with partially shrunken and collapsed structures. These observations suggest that *P5CR* also influences the growth, reproduction, and metabolic processes of *A. oxytropis* OW7.8.

Transcriptomic data suggest that SW biosynthesis in *A. oxytropis* OW7.8 is associated with pathways related to alkaloid and derivative metabolism, organic nitrogen compound metabolism, heterocyclic compound metabolism, terpenoid and polyketide metabolism, arginine and proline metabolism, secondary metabolite biosynthesis, and lysine biosynthesis and degradation. Among the DEGs in *A. oxytropis* OW7.8 and $\Delta P5CR$, six genes closely associated with SW biosynthesis (*swnN*, *swnR*, *swnK*, *swnH1*, *Aminoadipate reductase*, and *sac*) were downregulated. The products of *swnN*, *swnR*, *swnK*, and *swnH1* catalyze reactions downstream of *P5CR*. The knockout of *P5CR* likely reduced L-PA formation, leading to the downregulation of these four genes. However, due to limitations in transcriptomic platforms, genes such as *AASS*, *L-lysyl-alpha-oxidase*, *lysDH*, and *Saccharopine oxidase* were not enriched.

The metabolomic analysis identified six metabolites closely associated with SW biosynthesis: saccharopine, L-PA, α -aminoadipic acid, L-lysine, L-proline, and L-glutamate. Among these, saccharopine, L-PA, α -aminoadipic acid, L-lysine, and L-proline were downregulated in $\Delta P5CR$. Saccharopine, α -aminoadipic acid, L-PA, and L-lysine are key precursors in the SW biosynthetic pathway. The inactivation of *P5CR* in $\Delta P5CR$ disrupted the con-

version of P6C to L-PA, leading to reduced SW levels and the downregulation of upstream metabolites (saccharopine, α -aminoadipic acid, and L-lysine). P5CR also catalyzes the synthesis of L-proline from P5C. In $\Delta P5CR$, the inability to convert P5C to L-proline resulted in reduced L-proline levels, while the glutamate-semialdehyde dehydrogenase-mediated conversion of P5C to L-glutamate led to upregulated L-glutamate levels. Additionally, other enzymes, such as SwnR, may participate in the conversion of P6C to L-PA. However, due to limitations in metabolite databases, intermediates such as 6-amino-2-oxohexanoate, P2C, and P6C were not detected.

Integrated transcriptomic and metabolomic analyses revealed that the downregulation of *Aminoadipate reductase* reduced α -aminoadipic acid levels, as this enzyme catalyzes the conversion of α -aminoadipic acid to α -aminoadipate semialdehyde. Similarly, the downregulation of *sac*, which catalyzes the synthesis of saccharopine from α -aminoadipate semialdehyde, may be attributed to reduced levels of this intermediate. The SW biosynthetic pathway predicted based on the transcriptomic and metabolomic data in this study is consistent with the pathway proposed in our latest research [27,28]. These findings deepen our understanding of the SW biosynthetic pathway in *A. oxytropis* OW7.8 and provide insights into the enzymatic reactions involved. In the future, as more SW biosynthetic genes are characterized, we hope to further elucidate and refine the SW biosynthetic pathway.

5. Conclusions

This study constructed the gene knockout mutant strain $\Delta P5CR$ of *A. oxytropis* OW7.8. Compared to OW7.8, the SW content in $\Delta P5CR$ was significantly reduced, indicating that the *P5CR* gene promotes SW biosynthesis. The mutant also exhibited an altered colony and mycelial morphology. Transcriptomic and metabolomic analyses of *A. oxytropis* OW7.8 and $\Delta P5CR$ identified six downregulated genes and six differentially expressed metabolites closely associated with SW biosynthesis. The predicted SW biosynthetic pathway based on these omics data is consistent with our recent findings. This research provides a foundation for elucidating the molecular mechanisms and metabolic pathways of SW biosynthesis in fungi, offering valuable insights for controlling SW in *Oxytropis glabra* and contributing to the conservation and sustainable management of grassland ecosystems.

Supplementary Materials: The following supporting information can be downloaded at: <https://www.mdpi.com/article/10.3390/biom15040460/s1>.

Author Contributions: Conceptualization, P.L.; methodology, P.L., F.Y. and Y.L. (Yinzhe Li); investigation, P.L., F.Y., Y.L. (Yinzhe Li), Y.W., F.G., B.Y., L.D., Y.L. (Yuling Li), and K.J.; data curation, F.Y., Y.L. (Yinzhe Li), P.L. and Y.W.; writing—original draft preparation, F.Y. and Y.L. (Yinzhe Li); writing—review and editing, P.L., F.Y. and Y.L. (Yinzhe Li); visualization, F.Y., Y.L. (Yinzhe Li), and Y.W.; supervision, P.L.; project administration, P.L. All authors have read and agreed to the published version of the manuscript.

Funding: This research was funded by National Natural Science Foundation of China (31960130; 30860049), Natural Science Foundation of Inner Mongolia Autonomous Region of China (2022MS03014), and Fundamental Research Funds for the Inner Mongolia Normal University (2022JBTD010).

Institutional Review Board Statement: Not applicable.

Informed Consent Statement: Not applicable.

Data Availability Statement: The data presented in this study are available on reasonable request from the corresponding author.

Conflicts of Interest: The authors declare no conflicts of interest.

References

1. Yu, Y.; Zhao, Q.; Wang, J.; Wang, J.; Wang, Y.; Song, Y.; Geng, G.; Li, Q. Swainsonine-Producing Fungal Endophytes from Major Locoweed Species in China. *Toxicon* **2010**, *56*, 330–338. [[CrossRef](#)] [[PubMed](#)]
2. Guo, C.; Zhang, L.; Zhao, Q.; Beckmann, M.; Phillips, H.; Meng, H.; Mo, C.; Mur, L.A.J.; He, W. Host-Species Variation and Environment Influence Endophyte Symbiosis and Mycotoxin Levels in Chinese *Oxytropis* Species. *Toxins* **2022**, *14*, 181. [[CrossRef](#)]
3. Fu, J.J.; Guo, Y.Z.; Huang, W.Y.; Guo, R.; Lu, H.; Wu, C.C.; Zhao, B.Y. The Distribution of Locoweed in Natural Grassland in the United States and the Current Status and Prospects of Research on Animal Poisoning. *Acta Agrestia Sin.* **2019**, *27*, 519–530.
4. Cook, D.; Gardner, D.R.; Lee, S.T.; Pfister, J.A.; Stonecipher, C.A.; Welsh, S.L. A Swainsonine Survey of North American *Astragalus* and *Oxytropis* Taxa Implicated as Locoweeds. *Toxicon* **2016**, *118*, 104–111. [[CrossRef](#)] [[PubMed](#)]
5. Molyneux, R.J.; McKenzie, R.A.; O’Sullivan, B.M.; Elbein, A.D. Identification of the Glycosidase Inhibitors Swainsonine and Calystegine B₂ in Weir Vine (*Ipomoea* SP. Q6 {AFF. CALOBRA}) and Correlation with Toxicity. *J. Nat. Prod.* **1995**, *58*, 878–886. [[CrossRef](#)] [[PubMed](#)]
6. Wang, S.; Tan, P.; Wang, H.; Wang, J.; Zhang, C.; Lu, H.; Zhao, B. Swainsonine inhibits autophagic degradation and causes cytotoxicity by reducing CTSD O-GlcNAcylation. *Chem.-Biol. Interact.* **2023**, *382*, 110629. [[CrossRef](#)]
7. Wang, H.; Liu, Y.-S.; Peng, Y.; Chen, W.; Dong, N.; Wu, Q.; Pan, B.; Wang, B.; Guo, W. Golgi α -mannosidases regulate cell surface N-glycan type and ectodomain shedding of the transmembrane protease corin. *J. Biol. Chem.* **2023**, *299*, 105211. [[CrossRef](#)]
8. Fu, K.; Chen, X.; Shou, N.; Wang, Z.; Yuan, X.; Wu, D.; Wang, Q.; Cheng, Y.; Ling, N.; Shi, Z. Swainsonine Induces Liver Inflammation in Mice via Disturbance of Gut Microbiota and Bile Acid Metabolism. *J. Agric. Food Chem.* **2023**, *71*, 1758–1767. [[CrossRef](#)]
9. Xin, L.; Ping, L. Advances in research on swainsonine biosynthesis pathway in fungi. *Chem. Life* **2018**, *38*, 815–820.
10. Cook, D.; Gardner, D.R.; Pfister, J.A. Swainsonine-Containing Plants and Their Relationship to Endophytic Fungi. *J. Agric. Food Chem.* **2014**, *62*, 7326–7334. [[CrossRef](#)]
11. Quach, Q.N.; Clay, K.; Lee, S.T.; Gardner, D.R.; Cook, D. Phylogenetic Patterns of Bioactive Secondary Metabolites Produced by Fungal Endosymbionts in Morning Glories (Ipomoeae, Convolvulaceae). *New Phytol.* **2023**, *238*, 1351–1361. [[CrossRef](#)] [[PubMed](#)]
12. Cook, D.; Donzelli, B.G.G.; Creamer, R.; Baucom, D.L.; Gardner, D.R.; Pan, J.; Moore, N.; Krasnoff, S.B.; Jaromczyk, J.W.; Schardl, C.L. Swainsonine Biosynthesis Genes in Diverse Symbiotic and Pathogenic Fungi. *G3 Genes Genomes Genet.* **2017**, *7*, 1791–1797.
13. Wang, C.; Liu, R.; Lim, G.-H.; De Lorenzo, L.; Yu, K.; Zhang, K.; Hunt, A.G.; Kachroo, A.; Kachroo, P. Pipecolic Acid Confers Systemic Immunity by Regulating Free Radicals. *Sci. Adv.* **2018**, *4*, eaar4509. [[PubMed](#)]
14. Gao, X.; Cook, D.; Ralphs, M.H.; Yan, L.; Gardner, D.R.; Lee, S.T.; Panter, K.E.; Han, B.; Zhao, M.-L. Detection of Swainsonine and Isolation of the Endophyte *Undifilum* from the Major Locoweeds in Inner Mongolia. *Biochem. Syst. Ecol.* **2012**, *45*, 79–85. [[CrossRef](#)]
15. Pryor, B.M.; Creamer, R.; Shoemaker, R.A.; McLain-Romero, J.; Hambleton, S. *Undifilum*, a New Genus for Endophytic *Embellisia Oxytropis* and Parasitic *Helminthosporium Bornmuelleri* on Legumes. *Botany* **2009**, *87*, 178–194. [[CrossRef](#)]
16. Baucom, D.L.; Romero, M.; Belfon, R.; Creamer, R. Two New Species of *Undifilum*, Fungal Endophytes of *Astragalus* (Locoweeds) in the United States. *Botany* **2012**, *90*, 866–875.
17. Braun, K.; Romero, J.; Liddell, C.; Creamer, R. Production of Swainsonine by Fungal Endophytes of Locoweed. *Mycol. Res.* **2003**, *107*, 980–988. [[CrossRef](#)]
18. Guan, H.; Liu, X.; Mur, L.A.J.; Fu, Y.; Wei, Y.; Wang, J.; He, W. Rethinking of the Roles of Endophyte Symbiosis and Mycotoxin in *Oxytropis* Plants. *J. Fungi* **2021**, *7*, 400. [[CrossRef](#)]
19. Yu, Y.T.; Wang, J.H.; Zhao, Q.M.; Li, H.L.; Song, Y.M.; Wang, Y.; Zhang, Z.; Cui, Z.; Geng, G.; Li, Q. Isolation and identification of swainsonine-producing fungal endophyte from *Oxytropis kansuensis*. *J. Northwest AF Univ.* **2009**, *37*, 40–46+51.
20. Wu, K.X.; Tang, S.Y.; Zhu, Y.R.; Guo, Z.Y.; Mo, C.H.; Zhao, B.Y.; Lu, H. Isolation and Identification of Endophytic Fungi from Wild-Type *Astragalus adsurgens* and Analysis of Swainsonine. *Acta Agrestia Sin.* **2022**, *30*, 1692–1700.
21. Zhang, L.; Wu, R. Assembly of High-quality Genomes of the Locoweed *Oxytropis Ochrocephala* and Its Endophyte *Alternaria Oxytropis* Provides New Evidence for Their Symbiotic Relationship and Swainsonine Biosynthesis. *Mol. Ecol. Resour.* **2023**, *23*, 253–272. [[CrossRef](#)] [[PubMed](#)]
22. Shi, M.; Li, Y.-Z. *Alternaria Gansuense*, a Plant Systematic Fungal Pathogen Producing Swainsonine In Vivo and In Vitro. *Curr. Microbiol.* **2023**, *80*, 232. [[CrossRef](#)] [[PubMed](#)]
23. Xin, L.; Ping, L. Transcriptome Profiles of *Alternaria Oxytropis* Provides Insights into Swainsonine Biosynthesis. *Sci. Rep.* **2019**, *9*, 6021.
24. Lu, P.; Li, X.; Wang, S.; Gao, F.; Bo, Y.; Xi, L.; Du, L.; Hu, J.; Zhao, L. Saccharopine Reductase Influences Production of Swainsonine in *Alternaria oxytropis*. *Sydowia* **2021**, *73*, 69–74.
25. Xi, L.J.; Lu, P.; Gao, F.; Du, L. The Influence of Different Additives on the Swainsonine Biosynthesis in Saccharopine Reductase Gene Disruption Mutant M1 of an Endophytic Fungus from *Oxytropis Glabra*. *Life Sci. Res.* **2018**, *22*, 298–304.
26. Muhammad, F.; Rafiq, A.; Muhammad, S.; Saad Ur, R.; Yasar, S.; Amjad, H.; Mohammad Maroof, S.; Amber, A.; Sabaz Ali, K. Real-time expression and in silico characterization of pea genes involved in salt and water-deficit stress. *Mol. Biol. Rep.* **2023**, *51*, 18.

27. Min, Y.; Yu, D.; Yang, J.; Zhao, W.; Zhang, L.; Bai, Y.; Guo, C. Bioinformatics and expression analysis of proline metabolism-related gene families in alfalfa under saline-alkali stress. *Plant Physiol. Biochem.* **2023**, *205*, 108182.
28. Shah, T.; Khan, Z.; Alahmadi Tahani, A.; Imran, A.; Asad, M.; Khan Shah, R.; Ansari Mohammad, J. Mycorrhizosphere bacteria inhibit chromium uptake and phytotoxicity by regulating proline metabolism, antioxidant defense system, and aquaporin gene expression in tomato. *Environ. Sci. Pollut. Res. Int.* **2024**, *31*, 24836–24850.
29. Zhou, B.; Zhang, T.; Wang, F. Unravelling the molecular and biochemical responses in cotton plants to biochar and biofertilizer amendments for Pb toxicity mitigation. *Environ. Sci. Pollut. Res. Int.* **2023**, *30*, 100799–100813.
30. Cook, D.; Beaulieu, W.T.; Mott, I.W.; Riet-Correa, F.; Gardner, D.R.; Grum, D.; Pfister, J.A.; Clay, K.; Marcolongo-Pereira, C. Production of the Alkaloid Swainsonine by a Fungal Endosymbiont of the Ascomycete Order Chaetothyriales in the Host *Ipomoea Carnea*. *J. Agric. Food Chem.* **2013**, *61*, 3797–3803.
31. Liu, C.; Ding, N.; Lu, P.; Yuan, B.; Li, Y.; Jiang, K. The Effects of *swnN* Gene Function of Endophytic Fungus *Alternaria Oxytropis* OW 7.8 on Its Swainsonine Biosynthesis. *Int. J. Mol. Sci.* **2024**, *25*, 10310. [[CrossRef](#)] [[PubMed](#)]
32. Li, D.; Zhao, X.; Lu, P.; Min, Y. The Effects of *swnH1* Gene Function of Endophytic Fungus *Alternaria Oxytropis* OW 7.8 on Its Swainsonine Biosynthesis. *Microorganisms* **2024**, *12*, 2081. [[CrossRef](#)]
33. Luo, F.; Hong, S.; Chen, B.; Yin, Y.; Tang, G.; Hu, F.; Zhang, H.; Wang, C. Unveiling of Swainsonine Biosynthesis via a Multibranching Pathway in Fungi. *ACS Chem. Biol.* **2020**, *15*, 2476–2484. [[PubMed](#)]
34. Wang, W.F.; Qian, Y.G.; Lu, P.; He, S.; Du, L.; Li, Y.L.; Gao, F. The Relationship between Swainsonine and Endophytic Fungi in Different Populations of *Oxytropis Glabra* from Inner Mongolia China. *J. Anim. Vet. Sci.* **2022**, *53*, 304–314.
35. Love, M.I.; Huber, W.; Anders, S. Moderated Estimation of Fold Change and Dispersion for RNA-Seq Data with DESeq2. *Genome Biol.* **2014**, *15*, 550.
36. Yu, G.; Wang, L.-G.; Han, Y.; He, Q.-Y. clusterProfiler: An R Package for Comparing Biological Themes Among Gene Clusters. *OMICS J. Integr. Biol.* **2012**, *16*, 284–287.
37. Young, M.D.; Wakefield, M.J.; Smyth, G.K.; Oshlack, A. Gene Ontology Analysis for RNA-Seq: Accounting for Selection Bias. *Genome Biol.* **2010**, *11*, R14.
38. Cooper, B.; Yang, R. An Assessment of AcquireX and Compound Discoverer Software 3.3 for Non-Targeted Metabolomics. *Sci. Rep.* **2024**, *14*, 4841. [[CrossRef](#)]
39. Sreekumar, A.; Poisson, L.M.; Rajendiran, T.M.; Khan, A.P.; Cao, Q.; Yu, J.; Laxman, B.; Mehra, R.; Lonigro, R.J.; Li, Y.; et al. Metabolomic Profiles Delineate Potential Role for Sarcosine in Prostate Cancer Progression. *Nature* **2009**, *457*, 910–914.
40. Haspel, J.A.; Chettimada, S.; Shaik, R.S.; Chu, J.-H.; Raby, B.A.; Cernadas, M.; Carey, V.; Process, V.; Hunninghake, G.M.; Ifedigbo, E.; et al. Circadian Rhythm Reprogramming during Lung Inflammation. *Nat. Commun.* **2014**, *5*, 4753.

Disclaimer/Publisher’s Note: The statements, opinions and data contained in all publications are solely those of the individual author(s) and contributor(s) and not of MDPI and/or the editor(s). MDPI and/or the editor(s) disclaim responsibility for any injury to people or property resulting from any ideas, methods, instructions or products referred to in the content.